Atomic-scale spin-wave polarizer based on a sharp antiferromagnetic domain wall

Ehsan Faridi,[1,*] Se Kwon Kim,[2] and Giovanni Vignale[1,†]
[1]*Department of Physics and Astronomy, University of Missouri, Columbia, Missouri 65211, USA*
[2]*Department of Physics, Korea Advanced Institute of Science and Technology, Daejeon 34141, Korea*

(Received 11 March 2022; revised 12 July 2022; accepted 26 August 2022; published 8 September 2022)

We theoretically study the scattering of spin waves from a sharp domain wall (DW) in an antiferromagnetic spin chain. While the continuum model for an antiferromagnetic material yields the well-known result that spin waves can pass through a wide DW with no reflection, here we show that, based on the discrete spin Hamiltonian, spin waves are generally reflected by a DW with a reflection coefficient that increases as the DW width decreases. Remarkably, we find that, in the interesting case of an atomically sharp DW, the reflection of spin waves exhibits strong dependence on the state of circular polarization of the spin waves, leading to mainly reflection for one polarization while permitting partial transmission for the other, thus realizing an atomic-scale spin-wave polarizer. The polarization of the transmitted spin wave depends on the orientation of the spin in the sharp DW, which can be controlled by an external field or spin torque. Our utilization of a sharp antiferromagnetic DW as an atomic-scale spin-wave polarizer leads us to envision that ultrasmall magnetic solitons such as DWs and skyrmions may enable realizations of atomic-scale spin-wave scatterers with useful functionalities.

DOI: 10.1103/PhysRevB.106.094411

I. INTRODUCTION

The propagation of spin waves in one-dimensional magnets is of great fundamental interest and is also relevant for the transport of information in magnetic nanostructures [1,2]. Compared to conventional electronic spin currents, spin waves in magnetic insulators hold the promise to reduce the energy dissipation owing to the absence of Joule heating. In addition, spin waves in antiferromagnetic materials naturally occur at higher frequency than ferromagnetic spin waves, raising hope for fast spintronic applications [3]. In contrast to ferromagnetic materials, where spin waves have only one state of circular polarization [4], antiferromagnetic materials host all types of polarization, ranging from circular to elliptical depending on hard-axis anisotropy [5–7].

The interaction between spin waves and spin textures such as DW has been studied extensively in the continuum micromagnetic approximation, where only wide DWs, much larger than the atomic scale, are considered [8–10]. It has been shown that in the absence of a magnetic field, spin waves experience negligible reflection over wide range of frequency when propagating on a static smooth DW [11,12]. Applying a magnetic field gives rise to a finite magnetization inside the DW, which results in a field-controlled reflection of spin waves from a DW [13]. In many studies the interaction between the spin wave and a DW is investigated as a new method to control the transmission of the spin wave [14–20].

The interaction between spin waves and a DW can be substantially different from that obtained in the continuum model as the DW becomes narrower. When the DW width is comparable to the lattice constant, the continuum approximation breaks down and thus the results obtained with the assumption of smooth textures can be invalidated [21]. For example, in a ferromagnetic spin chain, it has been shown that spin waves experience strong reflection from a narrow DW, even in the absence of an external field [22]. However, an analogous investigation has not been conducted for an antiferromagnetic narrow DW.

Recently, atomically sharp DWs have been observed by electron microscopy in antiferromagnet CuMnAs, and their existence is found to be consistent with density functional theory DFT calculations [23]. These findings motivate us to pursue the study of the interaction between spin waves and antiferromagnetic DW within a discrete spin chain model, which allows us to treat atomically sharp DWs.

The fundamental difference between smooth and sharp antiferromagnetic DWs is that the latter can be viewed as a pointlike ferromagnetic insertion in an otherwise regular antiferromagnetic spin structure. (Similarly, a sharp ferromagnetic DW can be viewed as a pointlike antiferromagnetic insertion in a regular ferromagnetic structure.)

In this paper we find that as the antiferromagnetic DW becomes atomically sharp, left-handed (LH) and right-handed (RH) spin waves get reflected with different amplitudes, depending on the orientation of the spins at the domain boundaries. Therefore such a sharp DW can act as a *polarizer* for spin waves, allowing spin waves of a given polarization to be transmitted much more efficiently than spin waves of the opposite polarization. Furthermore, the selectivity of the polarizer can be reversed by reversing the orientation of the spins at the domain boundaries. Lastly, we show that the selectivity of the spin polarizer is a function of the magnetic anisotropy field and tends to vanish when the latter increases.

This paper is organized as follows: The model and the theoretical formulation of the problem are outlined in Sec. II. In Sec. III we present the numerical results for the transmission /

*efbmm@mail.missouri.edu
†vignaleg@missouri.com

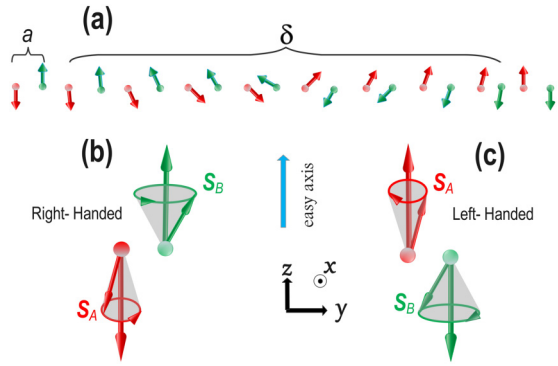

FIG. 1. (a) Schematic of a Néel DW with a width δ. Red (green) arrows represent sublattice A (B). Schematic of (b) RH and (c) LH eigenmode. Notice that in an RH wave the amplitude of oscillations on the sublattice with up-spin is larger than on the sublattice with down-spin. This causes the RH wave to carry a small net spin in the negative z direction. For LH waves the situation is reversed.

reflection probabilities of antiferromagnetic spin waves from a DW with an easy axis anisotropy. The transmission coefficients are shown to depend on the spin-wave wave vector and on its circular polarization. Here we also discuss the impact of changing magnetic anisotropy on the transmission of spin waves through the DW. Technical details are presented in the Appendixes.

II. THEORETICAL FORMULATION

A. Hamiltonian

Our starting point is a quasi-1D antiferromagnetic nanowire with a lattice spacing a in which a DW separates two homogeneous antiferromagnetic domains on the y axis. A sketch of a Néel-type antiferromagnetic DW with two arrows indicating two oppositely oriented spins on each sublattice is shown in Fig. 1(a). We consider an atomistic Heisenberg Hamiltonian of the form

$$\mathcal{H} = J\sum_n \mathbf{S}_n \cdot \mathbf{S}_{n+1} - D\sum_n \left(S_z^n\right)^2, \tag{1}$$

where S_n is the spin on the site n. The first term describes the isotropic exchange interaction between neighboring spins: for $J > 0$ this favors antiparallel alignment of neighboring spins. The second term, with $D > 0$, describes a uniaxial magnetic anisotropy, which favors the alignment of the spins along the z axis.

The equilibrium configuration of a DW between two uniform antiferromagnetic regions can be obtained by minimizing the energy with respect to a set of angles θ_n describing the equilibrium orientation of $\mathbf{S}_n$ relative to the z axis in the (z, y) plane (we assume that the DW lies entirely in this plane). Requiring the energy to be stationary with respect to infinitesimal variations of θ_n yields the equations

$$\sin(\theta_n - \theta_{n-1}) + \sin(\theta_n - \theta_{n+1}) - \frac{D}{J}\sin(2\theta_n) = 0. \tag{2}$$

To solve Eq. (2), we imposed the boundary condition that the spins on opposite sides of the DW region are in the z direction [see Fig. 1(a)]. For small values of the anisotropy, i.e., $D/J \ll 1$, Eq. (2) can be solved analytically using the approximation $||\theta_{n+1} - \theta_n| - \pi| \ll 1$. The solution has the form of an antiferromagnetic Walker-type profile. As the anisotropy increases, the DW starts to shrink, and for $D/J = 2/3$ the spins stay close to their anisotropy axis, forming an abruptly sharp DW.

In order to construct a linearized equation of motion for spin excitations on top of the DW, it is convenient to write the Hamiltonian in a local coordinate system which is rotated about the x axis in such a way that the local Z axis coincides with the local orientation of $\mathbf{S}_n$ at equilibrium.

The relation between the components of the spin in the local coordinate system (X, Y, Z) and in the global coordinate system (x, y, z) is

$$\begin{pmatrix} S_{nx} \\ S_{ny} \\ S_{nz} \end{pmatrix} = \begin{pmatrix} 1 & 0 & 0 \\ 0 & \cos\theta_n & \sin\theta_n \\ 0 & -\sin\theta_n & \cos\theta_n \end{pmatrix} \begin{pmatrix} S_{nX} \\ S_{nY} \\ S_{nZ} \end{pmatrix}. \tag{3}$$

We assume that the magnitudes of S_{nX} and S_{nY} (i.e., the nonequilibrium components of the spin in the local reference frame) are small in comparison with the magnitude of the spin on site n: $|S_{nX}|, |S_{nY}| \ll |S_{nZ}|$. Expanding to second order in S_{nX} and S_{nY}, the Hamiltonian takes the form

$$\begin{aligned} \mathcal{H} = J\sum_n & S_{nX}S_{n+1X} \\ & + \cos(\theta_n - \theta_{n+1})(S_{nY}S_{n+1Y} + S_{nZ}S_{n+1Z}) \\ & + \sin(\theta_n - \theta_{n+1})(S_{nY}S_{n+1Z} - S_{nZ}S_{n+1Y}) \\ & - D(S_{nZ}\cos\theta_n - S_{nY}\sin\theta_n)^2, \end{aligned} \tag{4}$$

Next, we perform the transformation

$$S_{nX} = \frac{S_{n+} + S_{n-}}{2}, \tag{5a}$$

$$S_{nY} = \frac{S_{n+} - S_{n-}}{2i}, \tag{5b}$$

$$S_{nZ} \approx S - \frac{S_{n-}S_{n+} + S_{n+}S_{n-}}{4S}, \tag{5c}$$

where S_{n+} and S_{n-} are the chiral components of the spin deviation [24]. This leaves us with a quadratic Hamiltonian of the form

$$\mathcal{H} \approx \sum_{n\alpha,n'\beta} h_{n\alpha,n'\beta}S_{n\alpha}S_{n'\beta}, \tag{6}$$

where α and β take values in $\{-, +\}$.

The site diagonal part $\mathcal{H}$ matrix is then given by

$$\begin{aligned} h_{n\alpha,n\beta} = & \left\{-J\frac{c_{n-1} + c_n}{4} + D\frac{2\cos^2\theta_n - \sin^2\theta_n}{4}\right\}[\sigma_x]_{\alpha\beta} \\ & + D\frac{\sin^2\theta_n}{4}\delta_{\alpha\beta}, \end{aligned} \tag{7}$$

and the off-diagonal parts are

$$h_{n\alpha,n+1\beta} = J\left(\frac{1 + c_n}{4}[\sigma_x]_{\alpha\beta} + \frac{1 - c_n}{4}\delta_{\alpha\beta}\right) \tag{8}$$

$$h_{n\alpha,n-1\beta} = J\left(\frac{1 + c_{n-1}}{4}[\sigma_x]_{\alpha\beta} + \frac{1 - c_{n-1}}{4}\delta_{\alpha\beta}\right), \tag{9}$$

where $c_n \equiv \cos(\theta_n - \theta_{n+1})$ and σ_i are the Pauli matrices.

B. Linearized equation of motion

Oscillations of the spin about the equilibrium DW configuration are governed by the equation of motion

$$\hbar \dot{S}_{n,\alpha} = i[\mathcal{H}, S_{n\alpha}], \tag{10}$$

which results in

$$-i\hbar\omega S_{n\alpha} = i \sum_{n'\beta,n''\gamma} h_{n'\beta,n''\gamma}\{[S_{n'\beta}, S_{n\alpha}] \times S_{n''\gamma} + S_{n'\beta}[S_{n''\gamma}, S_{n\alpha}]\}. \tag{11}$$

By using the Poisson bracket (or commutator) $[S_{n\alpha}, S_{n'\beta}] = -2S_{nZ}\epsilon_{\alpha\beta}\delta_{n,n'}$, where $\epsilon_{\alpha\gamma} = i[\sigma_y]_{\alpha\gamma}$, and replacing S_{nZ} by its equilibrium value, we obtain the linearized equation of motion for small oscillation about the equilibrium DW configuration:

$$\hbar\omega S_{n\alpha} = \sum_{n'\alpha\beta} H_{n\alpha,n'\beta} S_{n'\beta}. \tag{12}$$

Here the diagonal part of the spin-wave Hamiltonian is expressed as

$$H_{n\alpha,n\beta} = -JS(c_{n-1} + c_n)[\sigma_z]_{\alpha\beta} + DS(2\cos^2\theta_n - \sin^2\theta_n)[\sigma_z]_{\alpha\beta} + DS\sin^2\theta_n[i\sigma_y]_{\alpha\beta}, \tag{13}$$

and the off-diagonal part is

$$H_{n\alpha,n+1\beta} = JS\left\{\frac{1+c_n}{2}[\sigma_z]_{\alpha\beta} + \frac{1-c_n}{2}[i\sigma_y]_{\alpha\beta}\right\},$$
$$H_{n\alpha,n-1\beta} = JS\left\{\frac{1+c_{n-1}}{2}[\sigma_z]_{\alpha\beta} + \frac{1-c_{n-1}}{2}[i\sigma_y]_{\alpha\beta}\right\}.$$

C. Spin waves in a uniform ground state

Before studying spin waves on top of a DW, let us begin by solving the equations of motion (12) for a homogeneous antiferromagnetic state, described by $\theta_n = 0$ for even n and $\theta_n = \pi$ for odd n. We find two orthogonal solutions in the form of plane waves. The right-handed solution (written in the chiral basis) is

$$\psi_k^{(RH)}(n) = \{u_{k,\uparrow}^{(RH)}\delta_{\bar{n},0} + u_{k,\downarrow}^{(RH)}\delta_{\bar{n},1}\}e^{ikna}, \tag{14}$$

where $\bar{n} \equiv \text{Mod[n, 2]}$ and

$$u_{k,\uparrow}^{(RH)} = N_{k,1}\begin{pmatrix}1\\0\end{pmatrix}, \quad u_{k,\downarrow}^{(RH)} = -N_{k,2}\begin{pmatrix}0\\1\end{pmatrix}. \tag{15}$$

Similarly, the left-handed solution is

$$\psi_k^{(LH)}(n) = \{u_{k,\uparrow}^{(LH)}\delta_{\bar{n},0} + u_{k,\downarrow}^{(LH)}\delta_{\bar{n},1}\}e^{ikna}, \tag{16}$$

where

$$u_{k,\uparrow}^{(LH)} = N_{k,2}\begin{pmatrix}0\\1\end{pmatrix}, \quad u_{k,\downarrow}^{(LH)} = -N_{k,1}\begin{pmatrix}1\\0\end{pmatrix}. \tag{17}$$

Here $\uparrow$ ($\downarrow$) refer to direction of the spins at the sublattice A(B), and $N_{k,1(2)} = \sqrt{\frac{4(J+D)\pm 2\hbar\omega_k}{\hbar\omega_k}}$ are the amplitudes of the oscillation on the sites with $\uparrow$ ($\downarrow$) spins in the RH eigenmode. In the absence of an external magnetic field, the two eigenmodes are degenerate with eigenvalue

$$\hbar\omega_k = 2\sqrt{D(2J+D) + J^2\sin^2 ka}. \tag{18}$$

In the RH mode, both up- and down-spins undergo a counterclockwise precession when viewed from the $+z$ direction with frequency ω_k. In the LH mode, they both undergo a clockwise rotation with the same frequency. A schematic illustration of two modes is shown in Fig. 1.

D. Scattering problem

We are now ready to formulate the scattering problem. Deep inside the region I, $n \leqslant 0$, where the spins at even sites point in the $+z$ direction and the spins at odd sites point in the $-z$ direction, the solution is taken to be of the following form:

$$\psi_k(n) = \{u_{k,\uparrow}^{(RH)}\delta_{\bar{n},0} + u_{k,\downarrow}^{(RH)}\delta_{\bar{n},1}\}e^{ikna} + r_1\{u_{-k,\uparrow}^{(RH)}\delta_{\bar{n},0} + u_{-k,\downarrow}^{(RH)}\delta_{\bar{n},1}\}e^{-ikna} + r_2\{u_{-k,\uparrow}^{(LH)}\delta_{\bar{n},0} + u_{-k,\downarrow}^{(LH)}\delta_{\bar{n},1}\}e^{-ikna}. \tag{19}$$

This is the superposition of an incoming RH wave from the left and two reflected waves with RH and LH polarizations. r_1 and r_2 are the two reflection amplitudes.

In region III, $n > 2N$, where $2N$ is the number of spins inside the DW, the spins at even sites point in the $-z$ direction, and the spins at odd sites point in the $+z$ direction. The solution in this region is

$$\psi_k(n) = t_1\{u_{k,\downarrow}^{(RH)}\delta_{\bar{n},0} + u_{k,\uparrow}^{(RH)}\delta_{\bar{n},1}\}e^{ikna} + t_2\{u_{k,\downarrow}^{(LH)}\delta_{\bar{n},0} + u_{k,\uparrow}^{(LH)}\delta_{\bar{n},1}\}e^{ikna}, \tag{20}$$

i.e., a superposition of two transmitted waves of RH and LH polarization. t_1 and t_2 are the two transmission amplitudes.

In the intermediate region II, defined by $0 < n \leqslant 2N$, the solution of Eq. (10) (with the known values of θ_n) is constructed numerically with boundary conditions imposed by the previous two equations (19) and (20) at $n = 0$ and $n = 2N + 1$. The reflection and transmission amplitudes are then obtained by requiring that Eq. (19) and Eq. (20) are satisfied at the two boundary points $n = 0$ and $n = 2N + 1$. In view of the two-component character of the solution, this gives four linear equations from which r_1, t_1, r_2, t_2 can be determined.

III. RESULTS AND DISCUSSION

A. Scattering of the spin wave from a wide DW

First, let us consider a weak anisotropy, $D/J \ll 1$, in which a DW involves spatially slowly varying spins. In this limit, the Néel order parameter $\mathbf{n} = \frac{\mathbf{S}_A - \mathbf{S}_B}{2}$ is a three-dimensional unit vector and a continuous function of the coordinate y. Assuming that, at equilibrium, n lies in the (y, z) plane, we represent the equilibrium configuration of the DW as $\mathbf{n}_{eq} = \sin(\theta)\mathbf{y} + \cos(\theta)\mathbf{z}$, where the angle between $\mathbf{n}$ and the z axis is $\theta = 2\arctan[\exp(y/\delta)]$, where $\delta = a\sqrt{J/2D}$ is the characteristic width of the DW [25].

The equation of motion for the spin wave can be recast as a Schrödinger equation in an effective (Poschl-Teller) potential [26]:

$$\frac{\hbar^2}{D^2}\frac{\partial^2\phi(y,t)}{\partial t^2} = \delta^2\frac{\partial^2\phi(y,t)}{\partial y^2} - \left[1 - 2\text{sech}^2\frac{y}{\delta}\right]\phi(y,t). \tag{21}$$

Here $\phi = n_X + in_Y$, and n_X, n_Y are two components of the Néel order parameter in a *local* coordinate system such that

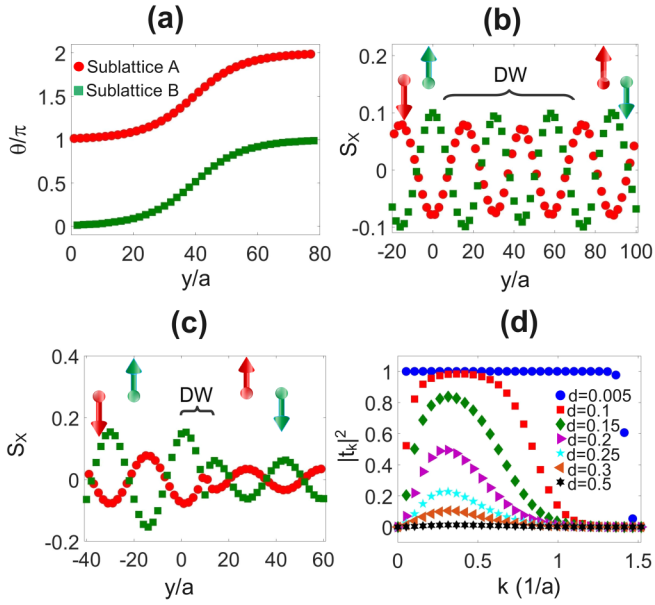

FIG. 2. (a) Exact DW profile with $d \equiv D/J = 0.005$. The red dots (green squares) represent the angles of spins at sublattice A (B). (b) Spin-wave profile for an incoming RH polarization with $k = 0.2$ and $d = 0.005$. The wave emerges with LH polarization on the other side of the DW. The arrows represent the direction of the equilibrium spin at sublattice A and B on both sides of the DW. (c) Spin-wave profile of an incoming RH polarization with $k = 0.2$ and $d = 0.2$. (d) Transmission coefficient of an incoming RH spin wave as a function of k for different values of d.

the Z axis (not to be confused with the absolute z axis) coincides with the direction of $\mathbf{n}_{\mathbf{eq}}$. The solution of this equation is

$$\phi(y,t) = \Phi \frac{\tanh\frac{y}{\delta} - i\delta k}{-1 - i\delta k} e^{-i\omega t + iky}, \quad \frac{\hbar^2\omega^2}{D^2} = 1 + (k\delta)^2, \tag{22}$$

which describes a circularly polarized wave of amplitude Φ. The profile of a spin wave on top of a wide DW is shown in Fig. 2(b). We see that an incoming RH spin wave passes through the DW without reflection and emerges on the other side with LH polarization [11,12]. We also notice that, in the left hand side of the DW, the amplitude of the oscillation on sublattice with up-spin (green square) is larger than that of sublattice with down-spin (red dots). The situation becomes reversed in the right-hand side of the DW, indicating a change of the polarization of the transmitted spin wave. Completely analogous results are obtained for an incoming LH polarization.

As D/J increases, the DW becomes progressively narrower and the continuum approximation breaks down. The numerical spin-wave solutions of an incoming RH spin wave for $D/J = 0.2$ and $k = 0.2$ are shown in Fig. 2(c). The RH spin wave is partially reflected without change in polarization. However, the transmitted spin wave absorbs spin angular momentum from the DW and reverses its polarization upon transmission [11,12]. The scenario for an incoming LH spin wave is similar. In this case the LH spin wave transfers spin angular momentum to the DW and emerges as a RH spin wave on the other side of the DW.

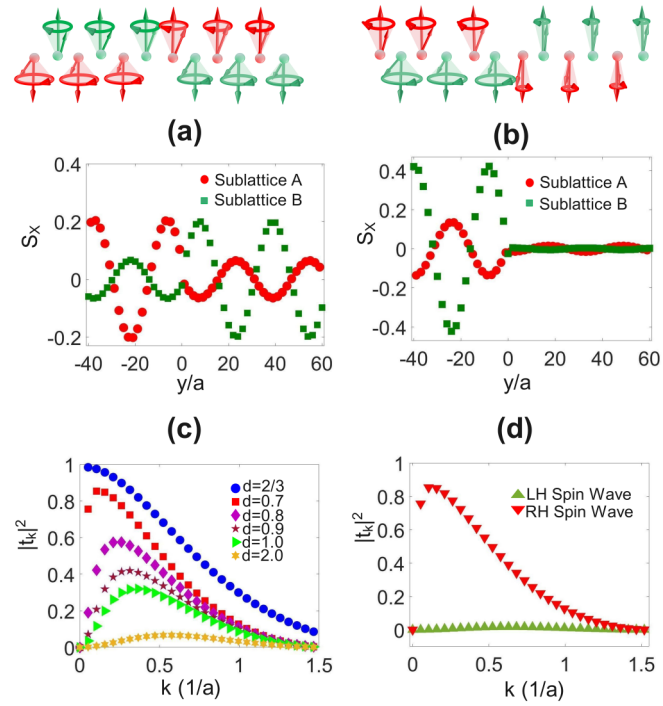

FIG. 3. (a) Spin-wave profile of an incoming LH polarization which scatters from an abruptly sharp DW with two up-spins at the domain boundaries at $d = 0.67$. The wave is transmitted with small reflection. (b) Same as in (a) for an abruptly sharp DW with two down-spins at the domain boundaries. Only a small portion of the wave is transmitted. (c) Transmission coefficient of an incoming LH spin wave scattered by two up-spins at the domain boundaries for different values of $D/J \equiv d$. (d) Transmission coefficient of an RH spin wave (red triangles) and an LH spin wave (green triangles) for an abruptly sharp DW with two down-spins at the domain boundaries as a function of k at $d = 0.7$.

The k-dependent transmission coefficient of an incoming RH spin wave is shown in Fig. 2(d) for different values of D/J. When $D/J \ll 1$, the transmission coefficient is $|t_k|^2 \approx 1$ for a wide range of k. For larger D/J the wave is partially reflected, and the transmission coefficients has a Gaussian-type shape with full width at half maximum in the range of $0.2 < k < 0.5$. This suggests that magnons with relatively large wave vector will dominate the spin transport in an uniaxial antiferromagnetic with large anisotropy.

B. Scattering of the spin wave from a sharp DW

Starting at $D/J = 2/3$ and for all larger values of D/J the equilibrium configuration of the DW becomes abruptly sharp and the scattering pattern of spin waves becomes different [27–30]. See Fig. 3 for the spin configurations of an abrupt DW. First of all, we notice that an abrupt DW, unlike a smooth one, has a net spin associated with it: we can regard it as a small ferromagnetic insertion in an antiferromagnetic background, and the spin of this insertion can point up or down. Second, the DW configuration is now invariant under rotations about the z axis, implying that different polarizations do not mix: an RH wave cannot be converted to an LH wave and vice versa; reflection and transmission amplitudes are

strictly diagonal in the polarization index. We will see that the transmission coefficient depends strongly on the polarization of the incoming wave relative to the orientation of spins at the domain boundaries.

The appeal of the sharp DW configuration is that it admits a completely analytical solution for the reflection and transmission amplitudes of spin waves. By substituting the Ansätze tze from Eq. (19) and Eq. (20) into Eq. (12) for an abrupt DW with two up-spins, the reflection and transmission amplitudes of an RH wave work out to be

$$r_k^{RH} = \frac{-1 + |\rho_k e^{-ika} - 2D/J + \hbar\omega_k/J|^2}{1 - (\rho_k e^{ika} - 2D/J + \hbar\omega_k/J)^2} \tag{23}$$

and

$$t_k^{RH} = \left(r_k^{RH} + e^{-2ika}\right)\rho_k - e^{-ika}\left(2\frac{D}{J} - \frac{\hbar\omega_k}{J}\right)\left(r_k^{RH} + 1\right), \tag{24}$$

where ω_k is the frequency of the incoming wave and $\rho_k = N_{k,2}/N_{k,1}$. For the same DW with two up-spins the reflection and transmission amplitudes of a LH wave are obtained by simply replacing $\omega_k \to -\omega_k$ in the above formulas, i.e., explicitly,

$$r_k^{LH} = \frac{-1 + |\rho_k^{-1} e^{-ika} - 2D/J - \hbar\omega_k/J|^2}{1 - \left(\rho_k^{-1} e^{ika} - 2D/J - \hbar\omega_k/J\right)^2} \tag{25}$$

and

$$t_k^{LH} = \left(r_k^{LH} + e^{-2ika}\right)\rho_k^{-1} - e^{-ika}\left(2\frac{D}{J} + \frac{\hbar\omega_k}{J}\right)\left(r_k^{LH} + 1\right). \tag{26}$$

The reflection and transmission amplitudes for a sharp DW with two down-spins at the boundaries can be obtained from the above results by interchanging the right-hand and the left-hand polarizations. The analytic expressions (23)–(26) for the reflection and transmission amplitudes of spin waves of two polarizations interacting with an abrupt antiferromagnetic DW are one of the main results of this paper.

Armed with these analytical results, we can easily plot the profile of spin waves as they get scattered by an abrupt DW. Let us first consider an incoming LH spin wave. As we can see in Fig. 3(a), for $k = 0.2$ and $D/J = 0.67$ the spin wave is transmitted through the DW without change in polarization. As D/J becomes larger, the transmission coefficient becomes smaller until, at $D/J \approx 4$, it becomes almost zero for the entire range of k [see Fig. 3(c)]. In contrast, for a sharp DW with two down-spins at the domain boundaries, the LH spin wave is mostly reflected for all values of k [Fig. 3(d)].

In the case of an incoming RH spin wave, the wave can be partially transmitted to the other side of a DW with two down-spins at the domain boundaries but is mostly reflected by a two up-spin DW. We see that changing the polarization of the incoming spin wave while simultaneously flipping the spins in the DW is a symmetry of the system.

We gain some insight into this surprising polarization dependence of the transmission coefficient by considering the analytic structure of the transmission amplitude for complex k (see Fig. 4). In the case of a DW with two up-spins at the domain boundaries the transmission amplitude for RH waves has two poles on the positive imaginary axis $k \to i\kappa$ with

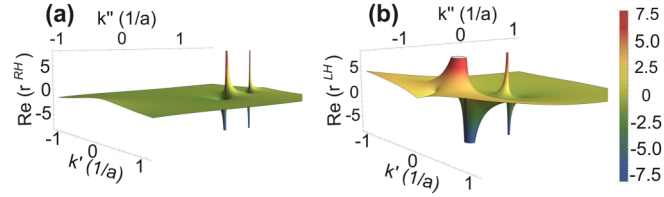

FIG. 4. (a, b) Real part of transmission amplitude of an incoming RH and LH spin waves in a complex plane respectively, i.e., $k = k' + ik''$ for $D/J = 1$.

$\kappa > 0$, which correspond to bound states, i.e., spin oscillations that are strongly localized on top of the sharp DW and decay exponentially away from the DW. These bound states are RH polarized, and their frequencies—obtained by substituting $k \to i\kappa$ in the formula for the spin-wave frequency—are given by

$$\hbar\omega_S = 2\sqrt{D(J+D)} \tag{27}$$

and

$$\hbar\omega_{AS} = \frac{-4J + \sqrt{36D^2 + 12DJ - 8J^2}}{3}, \tag{28}$$

where the subscript S refers to symmetric oscillation of the spins (i.e., the two spins at the domain boundaries rotate in phase), while the subscript AS refers to antisymmetric oscillations of the spins (i.e., the two spins at the domain boundaries rotate with a π phase difference between them). Notice that the antisymmetric mode frequency vanishes at $D/J = 2/3$.

The transmission amplitude for LH waves has no simple poles on the positive imaginary k axis, but it does have two poles on the negative imaginary k axis, i.e., at $k = i\kappa$, with $\kappa < 0$. The associated frequencies of these two poles are

$$\hbar\omega_{R1} = \frac{4J + \sqrt{36D^2 + 12DJ - 8J^2}}{3}, \quad \hbar\omega_{R2} = \hbar\omega_S. \tag{29}$$

What is the physical meaning of these two poles on the negative imaginary k axis? They are not bound states, because the associated solution of the equation of motion would diverge exponentially away from the DW. Nevertheless, the existence of such poles can have a large impact on the transmission coefficient if the pole occurs sufficiently near to the real axis [31–34]. When this happens, the pole is described as a *resonance*, meaning that it can cause a rapid increase of the transmission coefficient in a relatively narrow range of real wave vectors close to the pole. How narrow this range depends on how close the pole is to the real axis. In the present case, the pole at ω_{R1} is associated with an imaginary wave vector that occurs extremely near to the real axis when D/J approaches $2/3$. This is the mathematical origin of the sharp peak in the transmission coefficient of LH waves for small real k and for D/J close to $2/3$. For larger real k and/or for $D/J \gg 2/3$, the resonance disappears, as we clearly see in the numerical results [Fig. 3(c)].

A more physical description of the phenomenon can be achieved by noting that for $D/J \to 2/3$ the resonant frequency ω_{R1} approaches the real spin-wave frequency $\omega_{k=0}$ (see Fig. 5). We can therefore say that for $D/J \approx 2/3$ and $k \approx 0$ the frequency of the incoming spin wave matches the

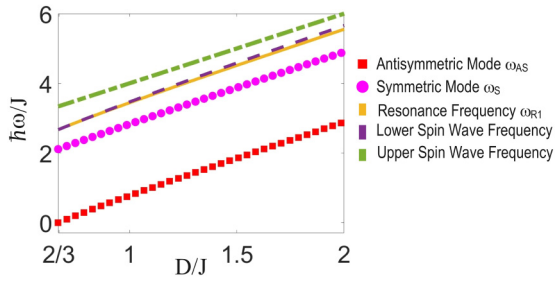

FIG. 5. Spin-wave frequency of a sharp DW as a function of D/J. Red squares show antisymmetric bound states, and purple circles show symmetric bound states. The yellow solid line shows the resonance frequency (ω_{R1}). The purple dashed line represents the lower bound of the continuous spin-wave frequency range, while the green dashed line represents the upper bound of that range.

frequency of the LH resonant state, resulting in a peak of the transmission coefficient.

To corroborate this point of view, we have derived an expression for the transmission probability of a spin wave in terms of bound states and resonance frequencies:

$$|t_k|^2 = \frac{J^2\big[(2D+2J)^2-\hbar^2\omega_k^2\big]\big[\hbar^2\omega_k^2-4D(D+2J)\big]}{3\hbar^4\big(\pm\omega_k^2-\omega_S^2\big)(\pm\omega_k-\omega_{AS})(\pm\omega_k+\omega_{R1})}, \tag{30}$$

where the upper sign applies to RH waves and the lower sign to LH waves. We emphasize that this expression is positive with values in the range $0 < |t_k|^2 < 1$ for all real k.

Now we can understand the selective transmission of spin waves according to their polarizations. In the case of incoming LH spin waves, and for $D/J \approx 2/3$, the spin-wave frequency, ω_k, stays close to the resonance frequency, i.e., for $\omega_k \approx \omega_{R1}$. Therefore the transmission probability becomes large [however, the vanishing numerator of Eq. (30) prevents divergence when $\omega_k = \omega_{R1}$]. As D/J increases, the difference between ω_k and ω_{R1} becomes larger, which results in a decreasing transmission probability. In contrast to LH, an RH spin wave of frequency ω_k never gets close to resonance due to the different sign in the denominator of Eq. (30): this explains the negligible transmission probability of RH spin waves.

Before concluding, a few comments are in order.

First of all, we note that in typical antiferromagnetic materials the anisotropy energy D tends to be quite smaller than $2/3$ of the exchange energy J, which is the critical value required for the appearance of abrupt DWs in our model. However, this is not a general rule. In fact, there are materials in which the anisotropy is much larger than exchange interaction. For example, the single ion anisotropy constant in FeI_2 has been experimentally measured to be one order of magnitude larger than the exchange constant [35].

Perhaps more importantly, in our work we focused on a simple model with uniform material constants to study the interaction of a spin wave with a sharp DW. In this model D/J is just the "knob" we turn to generate an abruptly sharp DW. However, a sharp DW can be formed when spatial inhomogeneities are present, e.g., where the spin environment spatially changes. In this latter case, our model is not suitable for a quantitative prediction of the interaction of spin waves and a DW, but we expect that our results will remain qualitatively valid regardless of the details of the DW formation mechanisms. In particular, we believe that the theoretical formalism developed in this work can be generalized to more complicated situations involving inhomogeneous material parameters, which we leave as a future research topic.

Lastly, we note that in an antiferromagnet the quantum fluctuations in the ground state can also be important, since the staggered magnetization is not a constant of the motion. However, in our model the large anisotropy produces a gap in the spin-wave frequency spectrum, which should ensure, even in a strictly one-dimensional case, that the fluctuation remains small.

IV. SUMMARY AND OUTLOOK

In conclusion, we have theoretically demonstrated that a sharp antiferromagnetic DW can act as a filter for the polarization of spin waves. As the DW becomes abruptly sharp, the state of circular polarization of an incoming wave (RH or LH) remains unchanged in the transmission/reflection process. For suitable values of the anisotropy parameter, the DW allows one of the two polarizations to pass while largely reflecting the other. A RH-polarized incoming spin wave gets mostly reflected by an abruptly sharp DW with two up-spins at the center, but it can be partially transmitted through a DW with two down-spins. Conversely, a LH-polarized incoming spin wave gets totally reflected by an abruptly sharp DW with two down-spins, but it can be partially transmitted through a DW with two up-spins. We understand these results in terms of resonant states (i.e., poles of the transmission amplitude for k close to the real axis but on the *negative* imaginary axis) whose frequency almost matches the frequency of the incoming wave. These resonances occur for one polarization but not for the other.

With an eye towards applications, these findings suggest that atomically sharp DWs can be used in magnonic circuits as spin polarizers.

ACKNOWLEDGMENTS

S.K.K. was supported by the Brain Pool Plus program through the National Research Foundation of Korea funded by the Ministry of Science and ICT (NRF-2020H1D3A2A03099291), by a National Research Foundation of Korea(NRF) grant funded by the Government of Korea (MSIT) (NRF-2021R1C1C1006273), and by the National Research Foundation of Korea funded by the Korea Government via the SRC Center for Quantum Coherence in Condensed Matter (NRF-2016R1A5A1008184).

APPENDIX A: ANTIFERROMAGNETIC SPIN WAVE—THE HOMOGENEOUS SOLUTION

In this Appendix we find the eigenfunctions and eigenvalues of a homogeneous antiferromagnetic structure. To do so, we set $\theta_n = \pi\bar{n}$, where $\bar{n} \equiv \text{Mod}[n, 2]$. This is 0 on the even sites and π on the odd sites. Then the spin-wave Hamiltonian

takes the form

$$\begin{aligned} H_{n\alpha,n\beta} &= \{2J+2D\}S[\sigma_z]_{\alpha\beta} \\ H_{n\alpha,n+1\beta} &= JS[i\sigma_y]_{\alpha\beta} \\ H_{n\alpha,n-1\beta} &= JS[i\sigma_y]_{\alpha\beta}. \end{aligned} \tag{A1}$$

The solution has the form

$$\psi_k(n) = u_k(n)e^{ikna}, \tag{A2}$$

where $u_k(n)$ is a two-component spinor which satisfies the periodicity condition $u_k(n+2) = u_k(n)$ and k is in the range $-\frac{\pi}{2a} < k < \frac{\pi}{2a}$. This means that $u_k(n)$ has only two distinct values, which we denote by $u_{k,0} \equiv u_k(0)$ and $u_{k,1} \equiv u_k(1)$. This function can be written as

$$u_k(n) = u_{k,0}\delta_{\bar{n},0} + u_{k,1}\delta_{\bar{n},1}. \tag{A3}$$

Notice that, with these definitions, we have

$$\psi_k(0) = u_{k,0}, \quad \psi_k(1) = u_{k,1}e^{ika}, \tag{A4}$$

where $u_{k,0}$ and $u_{k,1}$ are determined by applying the equation of motion to the sites $n = 0$ and $n = 1$ in the unit cell. Thus we get

$$\hbar\omega_k u_{k,0} = 2(J+D)\sigma_z u_{k,0} + 2J\cos(ka)(i\sigma_y)u_{k,1}, \tag{A5}$$

and

$$\hbar\omega_k u_{k,1} = 2(J+D)\sigma_z u_{k,1} + 2J\cos(ka)(i\sigma_y)u_{k,0}\,. \tag{A6}$$

We have two doubly degenerate eigenvalues

$$\hbar\omega_k = \pm 2\sqrt{D(2J+D) + J^2\sin^2 ka}. \tag{A7}$$

A possible choice of degenerate eigenvectors (for positive frequency) is

$$u^{(RH)}_{k,0} \equiv u^{(RH)}_{k,\uparrow} = N_{k,1}\begin{pmatrix}1\\0\end{pmatrix} \tag{A8a}$$

$$u^{(RH)}_{k,1} \equiv u^{(RH)}_{k,\downarrow} = -N_{k,2}\begin{pmatrix}0\\1\end{pmatrix}, \tag{A8b}$$

and

$$u^{(LH)}_{k,0} \equiv u^{(LH)}_{k,\uparrow} = N_{k,2}\begin{pmatrix}0\\1\end{pmatrix} \tag{A9a}$$

$$u^{(LH)}_{k,1} \equiv u^{(LH)}_{k,\downarrow} = -N_{k,1}\begin{pmatrix}1\\0\end{pmatrix}. \tag{A9b}$$

APPENDIX B: SPIN-WAVE SOLUTION FOR INHOMOGENEOUS SPIN CHAIN

Here we illustrate the numerical method for solving the equation of motion in the inhomogeneous region (DW). The DW includes the sites $n = 1, ..., 2N$, where the values of θ_n are already determined from Eq. (2). We first show that the amplitudes $\psi_1, ..., \psi_{2N}$ can be expressed as linear functions of ψ_0 and ψ_{2N+1}.

To this end we define the propagator

$$G = (\hbar\omega\tilde{1} - \tilde{H})^{-1}, \tag{B1}$$

where $\tilde{1}$ is a $4N \times 4N$ identity matrix and $\tilde{H}$ (also a $4N \times 4N$ matrix) is the restriction of the Hamiltonian to the subspace of the transition sites 1, ..., $2N$. Then, for $1 \leqslant n \leqslant 2N$ we have

$$\psi_n = G_{n,2N}H_{2N,2N+1}\psi_{2N+1} + G_{n,1}H_{1,0}\psi_0, \quad 1 \leqslant n \leqslant 2N. \tag{B2}$$

In addition, the solutions for ψ_n in the $n \leqslant 0$ and $n \geqslant 2N+1$ are given by Eqs. (19) and (20), respectively.

These formulas guarantee that the equation of motion is satisfied identically (i.e., for any choice of r_1, t_1, r_2, t_2) at almost every site, with the exception of the two sites $n = 0$ and $n = 2N+1$. On these special "frontier" sites the equation of motion is satisfied only for a specific choice of r_1, t_1, r_2, t_2. Thus the equations that determine the four scattering amplitudes are

$$(\hbar\omega - H_{0,0})\psi_0 - H_{0,-1}\psi_{-1} - H_{0,1}\psi_1 = 0 \tag{B3a}$$

and

$$\begin{aligned}(\hbar\omega - H_{2N+1,2N+1})\psi_{2N+1} - H_{2N+1,2N}\psi_{2N} \\ - H_{2N+1,2N+2}\psi_{2N+2} = 0.\end{aligned} \tag{B3b}$$

Let us insert the formulas for ψ_1 and ψ_{2N}:

$$\psi_1 = G_{1,2N}H_{2N,2N+1}\psi_{2N+1} + G_{1,1}H_{1,0}\psi_0, \tag{B4a}$$

$$\psi_{2N} = G_{2N,2N}H_{2N,2N+1}\psi_{2N+1} + G_{2N,1}H_{1,0}\psi_0. \tag{B4b}$$

This gives us the equations

$$\begin{aligned}(\hbar\omega - H_{0,0} - H_{0,1}G_{1,1}H_{1,0})\psi_0 - H_{0,-1}\psi_{-1} \\ - H_{0,1}G_{1,N}H_{N,N+1}\psi_{N+1} = 0\end{aligned}$$

and

$$\begin{aligned}(\hbar\omega - H_{2N+1,2N+1} \\ - H_{2N+1,2N}G_{2N,2N}H_{2N,2N+1})\psi_{2N+1} \\ - H_{2N+1,n}G_{2N,1}H_{1,0}\psi_0 - H_{2N+1,2N+2}\psi_{2N+2} = 0.\end{aligned}$$

All the quantities that appear in these equations are expressed in terms of r_1, t_1, r_2, t_2, and there are four equations because ψ is a two-component spinor. These equations can be solved to yield the scattering amplitudes.

APPENDIX C: BOUND STATES

In order to obtain an expression for each of the two bound-state frequencies, first we introduce the Ansatz for $n \leqslant 0$:

$$\begin{aligned}\psi_n(\kappa) = r_1\{u^{(RH)}_{\kappa,\uparrow}\delta_{\bar{n},0} + u^{(RH)}_{\kappa,\downarrow}\delta_{\bar{n},1}\}e^{\kappa na} \\ + r_2\{u^{(LH)}_{\kappa,\uparrow}\delta_{\bar{n},0} + u^{(LH)}_{\kappa,\downarrow}\delta_{\bar{n},1}\}e^{\kappa na},\end{aligned} \tag{C1}$$

and for $n \geqslant 1$,

$$\begin{aligned}\psi_n(\kappa) = t_1\{u^{(RH)}_{\kappa,\downarrow}\delta_{\bar{n},0} + u^{(RH)}_{\kappa,\uparrow}\delta_{\bar{n},1}\}e^{-\kappa na} \\ + t_2\{u^{(LH)}_{\kappa,\downarrow}\delta_{\bar{n},0} + u^{(LH)}_{\kappa,\uparrow}\delta_{\bar{n},1}\}e^{-\kappa na}.\end{aligned}$$

These are obtained by replacing $k \to i\kappa$ in Eq. (19).

By substituting Eq. (C1) as well as the dispersion relation of an evanescent wave, $\hbar\omega_\kappa = 2\sqrt{D(2J+D) - J^2\sinh^2\kappa a}$, in Eq. (12) with $n = 0$ we obtain

$$H_{0\alpha,0\beta}\psi_0 + H_{0\alpha,-1\beta}\psi_{-1} + H_{0\alpha,1\beta}\psi_1 = \hbar\omega\psi_0. \tag{C2}$$

The two spins at the domain boundaries can oscillate symmetrically or antisymmetrically relative to each other. In the

symmetric mode, the two spins oscillate with the same amplitude and with the same phase ($\psi_0 = \psi_1$), while in the antisymmetric mode they oscillate with the same amplitude but with opposite phase ($\psi_0 = -\psi_1$). Then Eq. (C2) can be simplified to

$$2\frac{D}{J}\sigma_z\psi_0 + i\sigma_y\psi_{-1} \pm \sigma_z\psi_0 = \frac{\hbar\omega}{J}\psi_0, \qquad n = 0, \tag{C3}$$

where (+) and (−) refer to symmetric and antisymmetric modes, respectively. Finally, the solution of Eq. (C3) gives the following expressions for the frequencies of the bound states:

$$\hbar\omega_{AS} = \frac{-4J + \sqrt{36D^2 + 12DJ - 8J^2}}{3} \tag{C4}$$

and

$$\hbar\omega_S = 2\sqrt{D(J+D)}, \tag{C5}$$

which agree with the numerical results shown in Fig. 5.

[1] T. Jungwirth, X. Marti, P. Wadley, and J. Wunderlich, Antiferromagnetic spintronics, Nat. Nanotechnol. **11**, 231 (2016).

[2] V. Baltz, A. Manchon, M. Tsoi, T. Moriyama, T. Ono, and Y. Tserkovnyak, Antiferromagnetic spintronics, Rev. Mod. Phys. **90**, 015005 (2018).

[3] J. Hortensius, D. Afanasiev, M. Matthiesen, R. Leenders, R. Citro, A. Kimel, R. Mikhaylovskiy, B. Ivanov, and A. Caviglia, Coherent spin-wave transport in an antiferromagnet, Nat. Phys. **17**, 1001 (2021).

[4] F. Keffer, H. Kaplan, and Y. Yafet, Spin waves in ferromagnetic and antiferromagnetic materials, Amer. J. Phys. **21**, 250 (1953).

[5] S. M. Rezende, A. Azevedo, and R. L. Rodríguez-Suárez, Introduction to antiferromagnetic magnons, J. Appl. Phys. **126**, 151101 (2019).

[6] R. Lebrun, A. Ross, O. Gomonay, V. Baltz, U. Ebels, A.-L. Barra, A. Qaiumzadeh, A. Brataas, J. Sinova, and M. Kläui, Long-distance spin-transport across the Morin phase transition up to room temperature in ultra-low damping single crystals of the antiferromagnet α-Fe2O3, Nat. Commun. **11**, 6332 (2020).

[7] A. Kamra, T. Wimmer, H. Huebl, and M. Althammer, Antiferromagnetic magnon pseudospin: Dynamics and diffusive transport, Phys. Rev. B **102**, 174445 (2020).

[8] A. C. Swaving and R. A. Duine, Current-induced torques in continuous antiferromagnetic textures, Phys. Rev. B **83**, 054428 (2011).

[9] P. Yan, X. S. Wang, and X. R. Wang, All-Magnonic Spin-Transfer Torque and Domain Wall Propagation, Phys. Rev. Lett. **107**, 177207 (2011).

[10] W. Wang, M. Albert, M. Beg, M.-A. Bisotti, D. Chernyshenko, D. Cortés-Ortuño, I. Hawke, and H. Fangohr, Magnon-Driven Domain-Wall Motion with the Dzyaloshinskii-Moriya Interaction, Phys. Rev. Lett. **114**, 087203 (2015).

[11] E. G. Tveten, A. Qaiumzadeh, and A. Brataas, Antiferromagnetic Domain Wall Motion Induced by Spin Waves, Phys. Rev. Lett. **112**, 147204 (2014).

[12] S. K. Kim, Y. Tserkovnyak, and O. Tchernyshyov, Propulsion of a domain wall in an antiferromagnet by magnons, Phys. Rev. B **90**, 104406 (2014).

[13] P. Shen, Y. Tserkovnyak, and S. K. Kim, Driving a magnetized domain wall in an antiferromagnet by magnons, J. Appl. Phys. **127**, 223905 (2020).

[14] J.-S. Kim, M. Stärk, M. Kläui, J. Yoon, C.-Y. You, L. Lopez-Diaz, and E. Martinez, Interaction between propagating spin waves and domain walls on a ferromagnetic nanowire, Phys. Rev. B **85**, 174428 (2012).

[15] S. Fukami, M. Yamanouchi, S. Ikeda, and H. Ohno, Depinning probability of a magnetic domain wall in nanowires by spin-polarized currents, Nat. Commun. **4**, 2293 (2013).

[16] S. Woo, T. Delaney, and G. S. Beach, Magnetic domain wall depinning assisted by spin wave bursts, Nat. Phys. **13**, 448 (2017).

[17] M. Voto, L. Lopez-Diaz, and E. Martinez, Pinned domain wall oscillator as a tuneable direct current spin wave emitter, Sci. Rep. **7**, 13559 (2017).

[18] S. J. Hämäläinen, M. Madami, H. Qin, G. Gubbiotti, and S. van Dijken, Control of spin-wave transmission by a programmable domain wall, Nat. Commun. **9**, 4853 (2018).

[19] J. Han, P. Zhang, Z. Bi, Y. Fan, T. S. Safi, J. Xiang, J. Finley, L. Fu, R. Cheng, and L. Liu, Birefringence-like spin transport via linearly polarized antiferromagnetic magnons, Nat. Nanotechnol. **15**, 563 (2020).

[20] J. Lan, W. Yu, and J. Xiao, Antiferromagnetic domain wall as spin wave polarizer and retarder, Nat. Commun. **8**, 178 (2017).

[21] H. Yang, H. Y. Yuan, M. Yan, H. W. Zhang, and P. Yan, Atomic antiferromagnetic domain wall propagation beyond the relativistic limit, Phys. Rev. B **100**, 024407 (2019).

[22] P. Yan and G. E. W. Bauer, Magnonic Domain Wall Heat Conductance in Ferromagnetic Wires, Phys. Rev. Lett. **109**, 087202 (2012).

[23] F. Krizek, S. Reimers, Z. Kašpar, A. Marmodoro, J. Michalička, O. Man, A. Edström, O. J. Amin, K. W. Edmonds, R. P. Campion *et al.*, Atomically sharp domain walls in an antiferromagnet, Sci. Adv. **8**, eabn3535 (2022).

[24] When the Hamiltonian is quantized, the operator S_{n+} creates a spin deviation at the site n, and the operator S_{n-} destroys it.

[25] E. G. Tveten, T. Müller, J. Linder, and A. Brataas, Intrinsic magnetization of antiferromagnetic textures, Phys. Rev. B **93**, 104408 (2016).

[26] A. V. Ferrer, P. F. Farinas, and A. O. Caldeira, One-Dimensional Gapless Magnons in a Single Anisotropic Ferromagnetic Nanolayer, Phys. Rev. Lett. **91**, 226803 (2003).

[27] B. Barbara, Propriétés des parois étroites dans les substances ferromagnétiques à forte anisotropie, J. Phys. **34**, 1039 (1973).

[28] J. Arnaudas, A. Del Moral, and J. Abell, Intrinsic coercive field in pseudobinary cubic intermetallic compounds. I. $Dy_xY_{1-x}Al_2$ and $Dy_{1-\delta}Al_2$, J. Magn. Magn. Mater. **61**, 370 (1986).

[29] H. Hilzinger and H. Kronmüller, Spin configuration and intrinsic coercive field of narrow domain walls in Co5R-compounds, Phys. Status Solidi B **54**, 593 (1972).

[30] B. Barbara, Magnetization processes in high anisotropy systems, J. Magn. Magn. Mater. **129**, 79 (1994).

[31] A. Kovalev, J. Prilepsky, E. Kryukov, and N. Kulik, Resonance properties of domain boundaries in quasi-two dimensional antiferromagnets, Low Temp. Phys. **36**, 831 (2010).

[32] T. Nakayama and S. Tsuchiya, Perfect transmission of Higgs modes via antibound states, Phys. Rev. A **100**, 063612 (2019).

[33] F. J. Buijnsters, A. Fasolino, and M. I. Katsnelson, Zero modes in magnetic systems: General theory and an efficient computational scheme, Phys. Rev. B **89**, 174433 (2014).

[34] E. Galkina and B. Ivanov, Dynamic solitons in antiferromagnets, Low Temp. Phys. **44**, 618 (2018).

[35] X. Bai, S.-S. Zhang, Z. Dun, H. Zhang, Q. Huang, H. Zhou, M. B. Stone, A. I. Kolesnikov, F. Ye, C. D. Batista *et al.*, Hybridized quadrupolar excitations in the spin-anisotropic frustrated magnet FeI_2, Nat. Phys. **17**, 467 (2021).